

Real time measurement of the emergence of superconducting order in a high temperature superconductor.

I. Madan¹, P. Kusar¹, V. V. Baranov¹, M. Lu-Dac¹, V. V. Kabanov¹, T. Mertelj¹, and D. Mihailovic^{1,2}

¹Complex Matter Department, Jozef Stefan Institute, and

²CENN Nanocentre, Jamova 39, 1000 Ljubljana, Slovenia

(Dated: October 25, 2018)

Systems which rapidly evolve through symmetry-breaking transitions on timescales comparable to the fluctuation timescale of the single-particle excitations may behave very differently than under controlled near-ergodic conditions. A real-time investigation with high temporal resolution may reveal new insights into the ordering through the transition that are not available in static experiments. We present an investigation of the system trajectory through a normal-to-superconductor transition in a prototype high-temperature superconducting cuprate in which such a situation occurs. Using a multiple pulse femtosecond spectroscopy technique we measure the system trajectory and time-evolution of the single-particle excitations through the transition in $\text{La}_{1.9}\text{Sr}_{0.1}\text{CuO}_4$ and compare the data to a simulation based on time-dependent Ginzburg-Landau theory, using laser excitation fluence as an adjustable parameter controlling the quench conditions in both experiment and theory. The comparison reveals the presence of significant superconducting fluctuations which precede the transition on short timescales. By including superconducting fluctuations as a seed for the growth of superconducting order we can obtain a satisfactory agreement of the theory with the experiment. Remarkably, the pseudogap excitations apparently play no role in this process.

The study of the time evolution of complex systems through symmetry breaking transitions (SBT) is of great fundamental interest in different areas of physics[1–3]. An SBT of particular general interest is the normal-to-superconducting ($N \rightarrow S$) state transition in which a Lorentz non-invariant system breaks gauge invariance.[4] By studying the $N \rightarrow S$ transition in time-evolving systems, rather than by slowly varying the temperature through the transition, one can in principle gain new information on the dynamical behavior of elementary excitations which lead to the formation of a superconducting condensate and the collective ordering behavior, leading to new insights into non-ergodic phenomena of collectively ordered systems as well as the mechanism of superconductivity. Particularly, ergodicity breaking in rapidly evolving systems leads to the appearance of topological defects (vortices).

The description of the dynamical behavior of the gauge non-invariant systems is given in the time-dependent Ginzburg-Landau theory (TDGL theory). It has been first applied to the problem of non-equilibrium phase transitions by Kibble and Zurek who considered the appearance of topological defects throughout the transition.[5, 6] The Kibble-Zurek description has been indirectly confirmed to be correct by static experiments in which trapped vortices were studied.[7, 8] In this paper, beyond previous static studies, we study *real-time evolution* of the superconducting order in the non-equilibrium phase transition. We investigate the applicability of TDGL theory to the phase transition problem and provide a minimal formulation sufficient to describe the data.

The paper is organized in the following way: we first introduce the problem of a non-homogeneous non-equilibrium phase transition, then present the three-pulse

technique we employed and describe acquired data. In the second half of the paper we present the numerical simulations of the $S \rightarrow N$ and $N \rightarrow S$ transitions with TDGL theory, using different formulation of the problem.

Laser induced nonequilibrium phase transition

An experimental realization of nonequilibrium conditions requires the inverse of the cooling rate - the quench time τ_q , to be comparable to the intrinsic collective system relaxation time $\tau_{\text{GL}} = \pi\hbar/8k(T-T_c) \simeq 10^{-13} - 10^{-12}$ s.[3, 9–11] So far the quench was physically limited to the ns timescale by heat diffusion processes or the duration of the optical pulse used for driving the transition.[8]

With femtosecond optical spectroscopy, nonequilibrium regime of the phase transition as well as measurements of the critical region in real time on the timescale of τ_{GL} become accessible. By properly adjusting pulse energy the limitations on the quench time set by heat diffusion processes can be overcome: for moderate fluences the electronic subsystem gets highly perturbed [12–14] while the lattice remains only weakly excited. In this case the cooling rate is defined by the energy exchange between electronic and lattice subsystems, which typically occurs on the sub-ps timescale[15], which is much faster than heat diffusion.

Optical experiments are intrinsically inhomogeneous due to finite light penetration depth λ_p . This affects not only the data analysis but also the physics of the transition. Due to the exponential depth-distribution of absorbed energy the superconducting condensate is destroyed only up to a certain depth. This results in a sharp boundary between the N and S states. After the quench the boundary propagates towards the surface and

is expected to reach it on a timescale $\tau_\psi \sim \lambda_p/v_\psi \sim \lambda_p\tau_{GL}/\xi_\perp \sim 10^3\tau_{GL}$, where v_ψ is the velocity of the S/N boundary[16] and ξ_\perp is the out-of-plane S coherence length. Though the boundary propagation is relatively slow, compared to τ_{GL} , the physics of the transition depends on how it relates to the propagation of the temperature front, which is defined by the quench conditions. Two regimes are possible: the temperature front propagation velocity v_T can be either larger (rapid quench) or smaller (slow quench) than the characteristic critical value $v_{crit} \approx v_\psi \sqrt{\tau_{GL}/\tau_q} \sim 10^5$ cm/s.[5] In the rapid quench limit when $v_T > v_{crit}$, the normal region between the temperature front and S/N boundary is supercooled and the order parameter grows from fluctuations. In this case one can expect vortex formation according to the Kibble-Zurek (KZ) mechanism. In the slow quench limit ($v_T < v_{crit}$) the condensate forms instantaneously in the wake of the temperature front so that the phase of the order parameter is defined by the bulk value and vortex formation becomes suppressed[5, 17].

As we shall see, both cases are accessible in our experiments via variable laser fluence: At low fluences, only the electrons are heated above T_c . They cool rapidly through T_c , so the quench rate $\gamma_q = (dT/dt)/T_c$ is fast[15]. With large fluences, the lattice is heated above T_c . Its cooling is defined by the heat diffusion so the quench rate is much slower.

Experimental results

To measure the trajectory of the system through the $N \rightarrow S$ transition, we use a 3 pulse technique shown schematically in Fig. 1 b). (See also Supplementary Information). The first, destruction (D) laser pulse strongly perturbs electronic subsystem initiating $S \rightarrow N$ transition on the timescale of ~ 0.8 ps.[12] The recovery of the S state in the ensuing $N \rightarrow S$ transition is measured by means of the pump-probe (P - pr) transient reflectivity $\Delta R(\Delta t_{P-pr})/R$ measurements. The pump-probe response is recorded at a set of delays Δt_{D-P} between D and P pulses[18]. For each value of the Δt_{D-P} delay the amplitude of the response $A = (\Delta R/R)^{max}$ is extracted, and, when plotted as a function of Δt_{D-P} , is a measure of the trajectory of the system. It is then compared to the modeled behavior of the order parameter $\psi(t)$ using an appropriate response function (See Supplement for a rigorous discussion).

We present measurements on a $\text{La}_{1.9}\text{Sr}_{0.1}\text{CuO}_4$ (LSCO) single crystal as a prototype single-layer cuprate well studied by means of pump-probe technique.[12, 19] The intermediate value of the $T_c = 28$ K is relatively high so that systematic with fluence experiments can be conducted, and simultaneously it is low enough so that the theoretical estimate of $\tau_{GL} \approx 100$ fs is longer than our resolution (30 fs). The laser fluence required

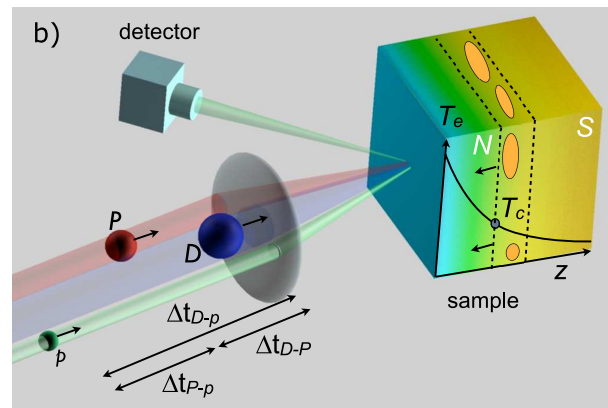
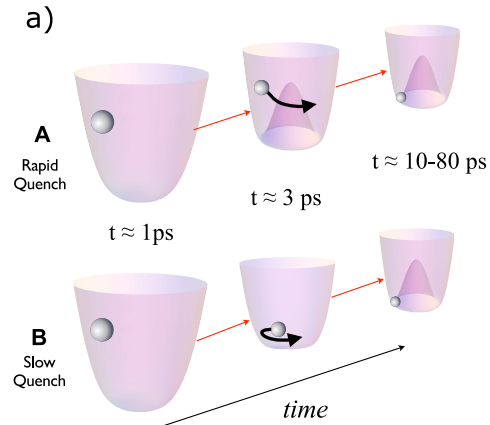


Figure 1. a) The system trajectory (depicted by the silver ball) in a temporally evolving potential. In the rapid quench scenario (A), the potential changes faster than the system can follow. The opposite is true in the slow quench scenario (B). b) A schematic diagram of the pulse sequence. The time delays Δt_{D-P} , Δt_{D-pr} and Δt_{P-pr} refer to delays between the D , P and pr pulses depicted in blue, red and green respectively. The S/N phase boundary moves with velocity v_ψ towards the surface. Vortices are created in the wake of the temperature front whose position is given by $T(r, t) = T_c$.

to destroy superconducting state on the surface (photodestruction threshold) has been previously determined to be $\mathcal{F}_T = 4.2 \pm 1.7 \mu\text{J}/\text{cm}^2$. [12] In the presented experiment we vary the D -pulse fluence from \mathcal{F}_T up to $34 \mu\text{J}/\text{cm}^2$.

A representative dataset obtained in a three-pulse experiment is shown in Fig. 2a). It depicts the transient reflectivity $\Delta R(\Delta t_{P-pr})/R$ traces for different Δt_{D-P} delays during the system recovery measured at 4K with D pulse fluence $\mathcal{F}_D = 12 \mu\text{J}/\text{cm}^2$. Two distinct and easily identifiable contributions are observed: a pseudogap (PG) response $(\Delta R/R)_{PG}$ which peaks around 0.2 ps,

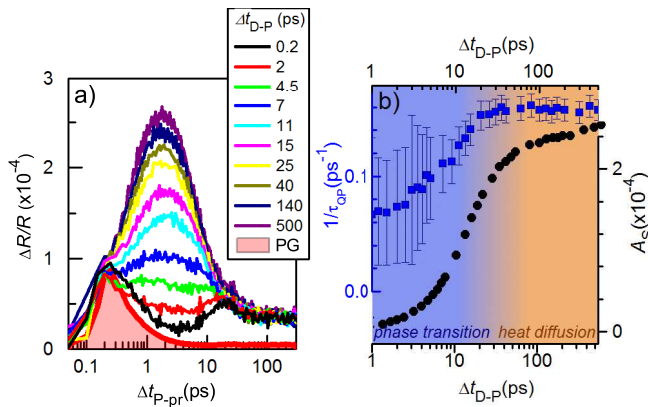


Figure 2. a) The transient reflectivity $\Delta R/R$ for $\text{La}_{1.9}\text{Sr}_{0.1}\text{CuO}_4$ at 4 K as a function of $\Delta t_{\text{D-pr}}$, for different $\Delta t_{\text{D-p}}$. The D pulse fluence is $\mathcal{F}_{\text{D}} = 12 \mu\text{J}/\text{cm}^2$, which is approximately three times above the destruction threshold ($\mathcal{F}_{\text{T}} \simeq 4 \mu\text{J}/\text{cm}^2$)[12]. The red line indicates the pseudogap signal measured above T_c . b) Black squares - the amplitude of the superconducting component A_S extracted from a) after subtraction of the PG. The blue squares are $1/\tau_{\text{QP}}$ as a function of $\Delta t_{\text{D-p}}$. The recovery of the system is schematically divided into phase transition region (blue background) where order parameter is not thermal, and into the thermal diffusion (orange background) where the transition is effectively over and order parameter is defined solely by the temperature.

and the quasiparticle (QP) recombination across the superconducting gap, i.e. the superconducting response $(\Delta R/R)_S$ which peaks near 2 ps, extending to tens of ps.[19, 20] We clearly observe that $(\Delta R/R)_S$ gradually increases with increasing delay $\Delta t_{\text{D-p}}$ indicating the recovery of the S state, while $(\Delta R/R)_{\text{PG}}$ remains intact by the destruction pulse and does not show any change with $\Delta t_{\text{D-p}}$.

$(\Delta R/R)_{\text{PG}}$ is known to be independent of T at temperatures below 100 K in this material.[19] We are interested in the superconducting order, so for further analysis we subtract it from the data [21] and plot the amplitude of the remaining superconducting response A_S as a function of $\Delta t_{\text{D-p}}$ in Fig. 2 b) (shown in black circles).

From the exponential fits of the initial decay of $(\Delta R/R)_S(\Delta t_{\text{D-pr}})$ we obtain the QP relaxation time τ_{QP} as a function of $\Delta t_{\text{D-p}}$ plotted in Fig 2 b).[22] We observe that $1/\tau_{\text{QP}}$ shows a similar to A_S time-evolution. If we assume that $1/\tau_{\text{QP}} \propto \Delta_S$, where Δ_S is the superconducting gap[23, 24], the observed dependence of τ_{QP} on $\Delta t_{\text{D-p}}$ is consistent with opening of the S gap for $\Delta t_{\text{D-p}} \sim 0$. The two variables A_S and τ_{QP} identify the recovery of superconducting order on a 10 ps timescale. The measured dependence of the trajectory $A_S(\Delta t_{\text{D-p}})$ for different fluences \mathcal{F} is shown in Fig. 4, where it is compared to the simulated trajectories from different models described below.

Modeling with time-dependent Ginzburg-Landau theory

In following we try to formulate the minimal TDGL theory which captures the observed behavior using laser pulse fluence as the only variable parameter. We consider only the real part of TDGL equations as the optical response is insensitive to the phase of the order parameter.[25] (In the supplement we solve the full set of TDGL equations to qualitatively account for dynamics of the phase and vortex dynamics.) The basic TDGL equation describing the order parameter $\psi(t, z)$ dynamics is [26]:

$$\frac{\partial \psi}{\partial t} = \alpha_r(t, z)\psi - \psi|\psi|^2 + \nabla^2 \psi, \quad (1)$$

where we have omitted explicit dependence of ψ on t and z , and the temporal and spatial coordinates are measured in units of τ_{GL} (fitting variable) and coherence length ($\xi = 0.2 \text{ nm}$ [27]) at $T = 0 \text{ K}$, respectively.

The system is driven by the electronic temperature T_e , which enters TDGL via $\alpha_r(t, z) = (1 - T_e(t, z)/T_c)$. The temperature is time dependent, and also depends on the depth in the sample. To calculate the actual shape of $T_e(t, z)$, we assume that electrons are preferentially coupled to a particular boson (phonon and/or spin excitation), which in turn releases its energy to the lattice. This three-temperature model (3TM) has been used in the past to describe the normal state ultrafast response in unconventional superconductors. [28, 29] In principle, the 3TM describes the destruction of the condensate, defines the recovery timescales and should also describe the slow diffusion processes clearly present in the data (Fig. 2 b). To account for the latter we introduce thermal diffusivity κ as a fitting parameter, which does not affect short timescales. The final set of the equations from which we obtain $T_e(t, z)$ is then:

$$\begin{aligned} \gamma_e T_e \dot{T}_e &= -\gamma_{\text{ep}}(T_e - T_p) + P(t) \\ C_p \dot{T}_p &= -\gamma_{\text{ep}}(T_p - T_e) - \gamma_{\text{pl}}(T_p - T_l) \\ C_l \dot{T}_l &= -\gamma_{\text{pl}}(T_l - T_p) + \kappa \frac{\partial^2 T_l}{\partial z^2}. \end{aligned} \quad (2)$$

where $\gamma_e = 2.5 \text{ mJ}/\text{mol}/\text{K}^2$ [30] is electronic specific heat coefficient, γ_{ij} represents the coupling between the i th and j th bath, T_i is the temperature of the corresponding system (indices e, p and l are for electronic, hot boson and lattice, respectively), and $P(t) = \frac{\mathcal{F}}{2\pi w} \exp(-t/2w^2) \exp(-z/\lambda)$ is the optical excitation, $w = 60 \text{ fs}$ is the pulse width at half maximum. We also assume that total phonon heat capacity $C = C_p + C_l$, where $C_p = \alpha C_0$ and $C_l = (1 - \alpha)C_0$ is heat capacity of hot bosons and the lattice bath, respectively, $\alpha = 0.2$ is a fraction of the phonons modes which are strongly coupled to electrons. [28] The coefficients of the 3TM model γ_{ep} and γ_{pl} can be estimated using electronic and

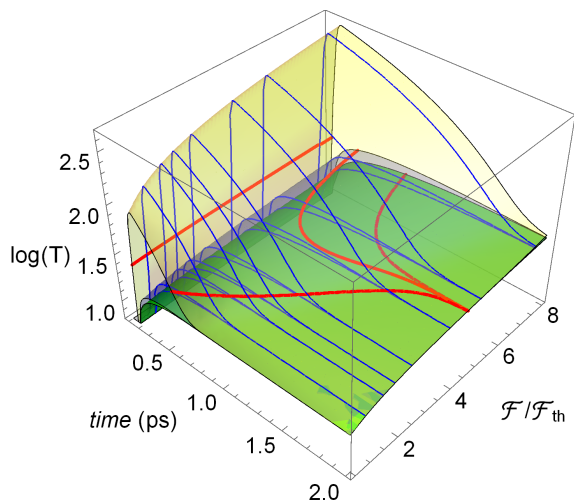


Figure 3. Three surfaces showing the calculated time evolution of the logarithm of T_e (yellow), T_p (blue) and T_l (green) as a function of incident fluence. The initial temperature of the sample is 4 K. T_p and T_l are very close, but T_e reaches in excess of 400 K. The blue lines correspond to fluences used in the experiment. The red lines indicate where T_e , T_p and T_l cross $T_c = 28$ K. T_e is used in the modeling of the order parameter. Fast quench corresponds to $\mathcal{F} < 5 \mathcal{F}_{th} \simeq 23 \mu\text{J}/\text{cm}^2$.

lattice thermal constants γ_e and C , measured electron-phonon relaxation rate $\gamma_l = 340\text{K}/\text{ps}$ and the phonon-phonon relaxation time $\tau_{ph} = 0.6$ ps [15]: $\gamma_{ep} = \gamma_e \gamma_l$ and $\gamma_{pl} = C_p / \tau_{ph}$. The temperature dependence of the phonon heat capacity C is obtained from published thermal data.[31]

Solving Eq. (2) we obtain the time and depth dependence of T_e , T_p and T_l . In Fig. 3 we plot the values of corresponding temperatures on the sample surface for different fluences used in the experiments. Initially, the pulse rapidly heats the electronic system, but energy is quickly transferred to the strongly coupled bosons and the lattice on a timescale ~ 1 ps, whereafter the three temperatures rapidly merge. Note that this timescale is of the same order as the destruction of the S state.[32] We see in Fig. 3 that for low excitation fluences $\mathcal{F}/\mathcal{F}_{th}$, the quench rate $\gamma_Q = (dT_e/dt)_{T_c}$ through T_c (red line) is fast, on the order of 4×10^{14} K/s and $T_e \simeq T_p \simeq T_l$ already after ~ 1 ps. With higher fluences, $> 5 \mathcal{F}_{th}$ when T_p and T_l both exceed the superconducting T_c , the cooling rate is mainly determined by thermal diffusion on timescales well beyond ~ 1 ps. We emphasize that this cross-over from rapid to slow quench is quite general and does not rely on the specific details of the 3TM. Having calculated $T_e(t, z)$, we can now calculate $\psi(t, z)$, and $A_S(t)$.

Within the **first approach** to the problem presented above, Eq. (1) describes *both* the destruction and recovery of the superconducting condensate. First we consider in detail the destruction stage, i.e. $S \rightarrow N$ transition. Initial conditions describe superconducting state in equi-

librium $\psi(0, z) = \sqrt{1 - T_{bath}/T_c}$. The transition is then driven by a temperature burst described by the α -term of Eq. (1). Within this approach the relation between τ_{GL} (the only free parameter) and duration of the temperature burst is crucial. For the condensate to be able to react to the intense short temperature perturbation τ_{GL} should be smaller than duration of perturbation ~ 1 ps. Such short τ_{GL} results also in rapid recovery, significantly faster than observed experimentally, as can be seen in Fig. 4 a) ($\tau_{GL} = 450$ fs). At fluences $\mathcal{F} \geq 18 \mu\text{J}/\text{cm}^2$ we enter the slow quench regime, i.e. perturbation duration is longer and OP suppression is more effective. This results in a recovery that occurs on the time-scale closer to experimentally observed.

On the other hand, if τ_{GL} is much longer than the perturbation, the condensate cannot follow the temperature dynamics and the condensate remains undestroyed. Thus the presented TDGL equations do not provide a good description of the destruction of the condensate. This can be easily understood as the destruction is the fastest of considered processes during which the distribution function is clearly not thermal which leads to effects which lie beyond a TDGL and 3TM description.[33]

To avoid the problem of the condensate photodestruction we focus on the recovery process, and define the state of the system after the $S \rightarrow N$ transition by the initial conditions. The solution of the TDGL equation then describes the ensuing recovery dynamics, i.e. the $N \rightarrow S$ transition. Within our **second approach** we determine initial depth-distribution of the condensate density from the fluence dependence of the amplitude in two pulse pump-probe response experiments[12]:

$$\psi(0, z) = \begin{cases} 0 & , \mathcal{F}(z) > \mathcal{F}_T; \\ (1 - \frac{\mathcal{F}}{\mathcal{F}_T} e^{-z/\lambda}) \sqrt{1 - \frac{T_1(0, z)}{T_c}} & , \mathcal{F}(z) < \mathcal{F}_T. \end{cases} \quad (3)$$

This expression can be considered as the limiting case of the fast quench without fluctuations. The solution of the TDGL equations then corresponds to an $S \rightarrow N$ boundary which moves towards the surface in the form of a S/N soliton wall without change of shape, and the recovery of the system is completely determined by the soliton propagation. This approach has only one free fit parameter τ_{GL} defining the velocity of the soliton v_s . By setting $\tau_{GL} = 50$ fs we obtain recovery on observable timescales. However, the obtained trajectories $A_S(\Delta t_{D-P})$ are much sharper than experimentally observed (Fig. 4 b). For the weakest excitation $\mathcal{F}(z=0) = \mathcal{F}_T = 4.2 \mu\text{J}/\text{cm}^2$ the condensate is destroyed only at the surface and recovery occurs in 50 fs. However, for the strongest excitation $\mathcal{F} = 34 \mu\text{J}/\text{cm}^2$ the slow quench condition is satisfied and the soliton follows the temperature front. In this case the simulated curve fits reasonably well to the data (Fig. 4 b).

The gradual growth of the S signal on the 10 ps

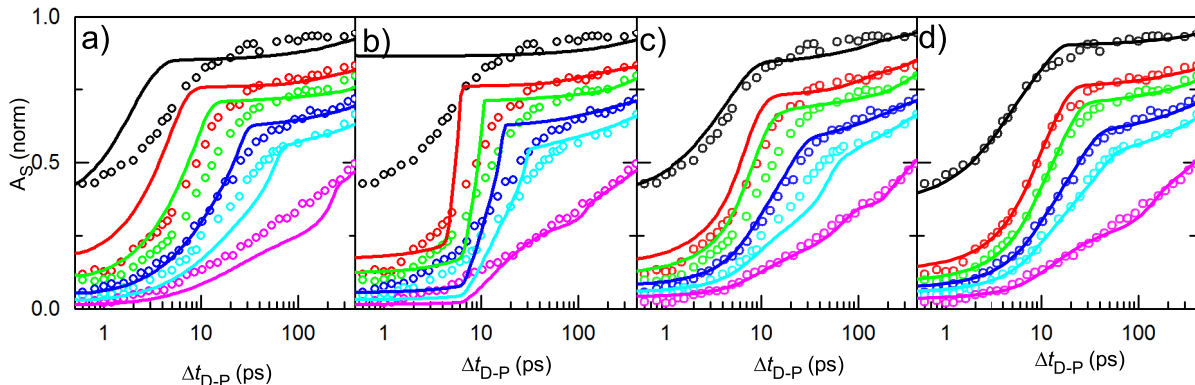


Figure 4. Comparison of experimentally measured data (circles, values of fluence are 4 (black), 9 (red), 12 (green), 18 (blue), 24 (cyan), and 34 (magenta) $\mu\text{J}/\text{cm}^2$) and the calculated A_S obtained within different formulation of problem (solid lines): TDGL solution with initial conditions described by a) $\psi(0, z) = \sqrt{1 - T_{\text{bath}}/T_c}$, b) Eq. 3, c) Eq. 4 (represented in Fig. 5), d) Eq. $\psi_{\text{fluc}}(0, z) = \kappa z$.

timescale for the intermediate fluences might be reproduced if one assumes that the main source of the emerging order is superconducting fluctuations along the Kibble-Zurek scenario. It has been widely discussed that cuprates have extremely strong fluctuations compared to conventional superconductors and their onset in certain families exceeds the critical temperature by several tens of K above T_c . [25, 34–37] Thus we expect to have a significant contribution from fluctuations and expect them to be an effective seed for the order parameter growth.

In a simple pre-formed pair scenario of superconductivity, the pseudogap energy corresponds to the pair formation energy. One thus can assume that superconductivity arises from pseudogap-forming carriers. Their density after the photoexcitation can be described by equation 3, where \mathcal{F}_T would now correspond to the pseudogap photodestruction fluence \mathcal{F}_{PG} . In LSCO this fluence is extremely high $\mathcal{F}_{PG} \sim 750 \pm 200 \mu\text{J}/\text{cm}^2$. [20] Under excitation conditions considered in this work $\mathcal{F} \leq 34 \mu\text{J}/\text{cm}^2$ pseudogap would hardly be affected at all, which is confirmed by the robustness of the PG response in three-pulse experiments. This implies that the initial conditions for equation (3) would be more or less constant with depth and fluence. Such fluence-independent initial conditions are inconsistent with the fluence-dependence of the data, so the PG does not appear to seed the S order parameter, and does not improve the model fit.

The third approach: thermal fluctuations. A more relevant scenario invokes fluctuations of the superconducting order above T_c . After the S order has been destroyed and the temperature is still significantly above T_c ($\Delta t_{D-P} \sim 0.2$ ps) weak short-lived superconducting fluctuations exist in the system. As the electronic sub-

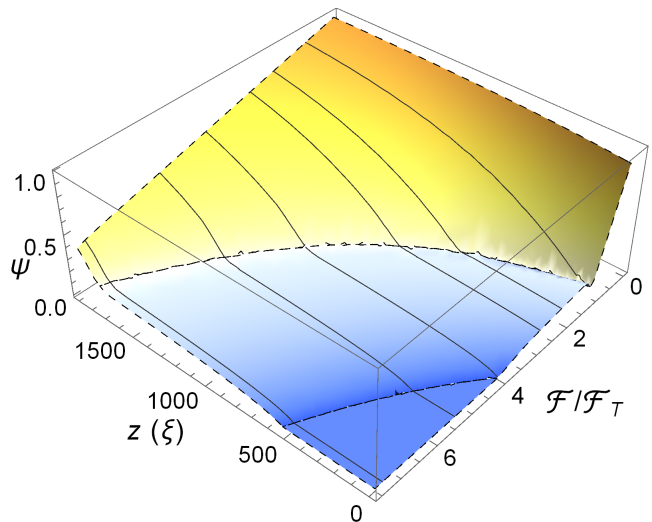


Figure 5. Initial condition that take into account fluctuations of the order parameter according to the Eq. (4) (blue surface) and partially suppressed (yellow surface) order parameter in the region $\mathcal{F}(z) < \mathcal{F}_T$. in agreement with Eq. (3).

system rapidly cools the density of the S fluctuations increases, and their lifetime and correlation length diverge as $T \rightarrow T_c$. During the initial cooling stage ($T \gg T_c$) fluctuations are fast and would adapt to the variation in temperature. However, after a certain moment in time given by $\tau_Z = \sqrt{\tau_{GL}\tau_q}$ their lifetime would become larger than the quench time, meaning that the system would cross the transition in a "frozen" inhomogeneous configuration. As the system escapes the critical region $T < T_c(1 - \frac{\tau_z}{\tau_q})$ the fluctuation lifetime decreases and

the system starts to adapt to the new conditions, i.e. the order parameter grows from fluctuations according to TDGL theory. The appropriate expression for such fluctuations, which we can implement as initial conditions have been given by Volovik [38][39]

$$\psi_{\text{fluc}}(0, z) \sim \left(\frac{\tau_{\text{GL}}}{\tau_{\text{q}}(z)} \right)^{3/8} \frac{T_{\text{c}}}{E_{\text{F}}} \psi_{\text{eq}}(T_{\text{i}}). \quad (4)$$

Factor $\frac{T_{\text{c}}}{E_{\text{F}}}$ gives the correct order of magnitude ~ 0.01 of the seed order parameter, whereas τ_{q} and $\psi_{\text{eq}}(T_{\text{i}})$ define the depth dependence. The spatial dependence of the initial order parameter is shown in Fig. 5. We note that the actual initial temperature after the photon absorption is not important because the properties of the seed OP are defined at $T_{\text{Z}} = T_{\text{c}}(1 + \frac{z}{\tau_{\text{q}}})$. For the initial condition of the equation (1) we use the equation (4) with the proportionality factor C : $\psi_{\text{ini}}(\mathcal{F}(z) > \mathcal{F}_{\text{T}}) = C \cdot \psi_{\text{fluc}}(0, z)$ which, together with τ_{GL} , was used as an adjustable parameter shared between all curves. The resulting trajectories are shown in Fig. 4 c) (parameter values are $\tau_{\text{GL}} = 1.25$ ps and $C = 4$). The agreement between experimental data and simulations is now much better.

Finally, we improve the fit by solving the TDGL equation with parametrized phenomenological initial conditions which resemble main feature of the Volovik's result i.e. growth of the fluctuations with depth. The goal here is to provide initial conditions where depth dependence is adjustable rather than defined by the quench-rate deduced from the 3TM which may not be sufficiently accurate. Instead of equation (4) we use the minimal model which produces a reliable fit: $\psi_{\text{fluc}}(0, z) = \kappa z / \lambda_{\text{p}}$, where κ is the fitting parameter independent for each fluence value. Result of this simulations is presented in Fig. 4 d) with κ values equal to 0.25, 0.23, 0.162, 0.13, 0.1 and 0.06 in the order of the increasing fluence, and $\tau_{\text{GL}} = 1.1$ ps. The good agreement of the simulation with the data justifies the initial conditions within the fluctuation scenario and underlines importance of the fluctuations especially for low and intermediate fluences.

We conclude that the evolution of the superconducting order through the non-equilibrium phase transition can be described quite well with time-dependent Ginzburg Landau theory. We show in the supplement that the remaining discrepancy between the fit and the data near ~ 10 ps for the two fastest quench rates can be accounted for by the suppression of the order parameter due to vortex formation. From the discussion above one can see that in the case of a fast quench the ergodicity of the system is broken as soon as the fluctuation timescale becomes longer than the quench time. The system then cannot follow the time-evolution of the potential and so evolves inhomogeneously through the transition with the creation of vortices, quite faithfully reproduced by the model when the dynamics of the superconducting phase is explicitly included in the calculations (Fig. 4 of the

supplement).

The fact that the *destruction* of the condensate cannot be properly described by TDGL equations is not surprising, particularly if we rely only on the 3TM, which does not take into account the details of the destruction process. On the other hand, in spite of all its inherent shortcomings, the ensuing recovery of S order predicted by the model agrees quite well with the experiments, and emphasizes a crucial role of fluctuations in the time-evolution of the order parameter through the $N \rightarrow S$ transition. Remarkably, the experiments show that the S order appears to grow out of the pseudogap state, yet from the strong fluence dependence of the S recovery and complete fluence-independence of the PG state we conclude that the pseudogap has no effect in seeding the emergence of the superconducting order.

We wish to acknowledge the useful discussion with T.W. Kibble regarding the importance of a variable quench rate in the experiment. The funding was provided by European Research Council advanced grant TRAJECTORY.

-
- [1] Y. M. Bunkov and H. Godfrin, *Topological Defects and the Non-Equilibrium Dynamics of Symmetry Breaking Phase Transitions*, edited by Y. M. Bunkov and H. Godfrin (Springer Netherlands, Dordrecht, 2000) p. 396.
 - [2] P. W. Higgs, *Physical Review* **145**, 1156 (1966).
 - [3] G. Volovik, *Contemporary Physics*, Vol. 51 (Oxford university press, 2010) pp. 451–452.
 - [4] C. M. Varma, *Journal of Low Temperature Physics* **126**, 901 (2002), arXiv:0109409 [cond-mat].
 - [5] T. W. B. Kibble and G. E. Volovik, *Journal of Experimental and Theoretical Physics* **65**, 102 (1997).
 - [6] W. Zurek, *Physics Reports* **276**, 177 (1996).
 - [7] R. Monaco, J. Mygind, M. Aaroe, R. Rivers, and V. Koshelets, *Physical Review Letters* **96**, 5 (2006).
 - [8] D. Golubchik, E. Polturak, and G. Koren, *Physical Review Letters* **104**, 1 (2010).
 - [9] W. H. Zurek, *Nature* **317**, 505 (1985).
 - [10] A. Schmid and G. Schön, *Journal of Low Temperature Physics* **20**, 207 (1975).
 - [11] A. Schmid, *Physik der Kondensierten Materie* **5**, 302 (1966).
 - [12] P. Kusar, V. V. Kabanov, J. Demsar, T. Mertelj, S. Sugai, and D. Mihailovic, *Physical Review Letters* **101**, 1 (2008).
 - [13] C. Giannetti, G. Coslovich, F. Cilento, G. Ferrini, H. Eisaki, N. Kaneko, M. Greven, and F. Parmigiani, *Physical Review B* **79**, 1 (2009).
 - [14] G. Coslovich, C. Giannetti, F. Cilento, S. Dal Conte, G. Ferrini, P. Galinetto, M. Greven, H. Eisaki, M. Raichle, R. Liang, A. Damascelli, and F. Parmigiani, *Physical Review B* **83**, 064519 (2011), arXiv:1005.4320.
 - [15] C. Gadermaier, A. Alexandrov, V. Kabanov, P. Kusar, T. Mertelj, X. Yao, C. Manzoni, D. Brida, G. Cerullo, and D. Mihailovic, *Physical Review Letters* **105**, 1 (2010).

- [16] The 1-D time dependent GL equation $\tau_{\text{GL}}\dot{\psi} = \xi^2\psi'' + (1 - T/T_c)\psi - \psi^3$ has a propagating soliton solution $\psi \propto \tanh[(v_\psi t - z)/w] - 1$ where $w = 2\sqrt{2}\xi/\sqrt{1 - T/T_c}$ and $v_\psi = 3\xi\sqrt{1 - T/T_c}/\sqrt{2}\tau_{\text{GL}}$. Taking $\xi \sim \xi_\perp \sim 0.2$ nm and $\tau_{\text{GL}} \sim 100$ fs gives $v_\psi < 5$ nm/ps..
- [17] I. S. Aranson, N. B. Kopnin, and V. M. Vinokur, *Physical Review Letters* **83**, 2600 (1999), arXiv:9905286 [cond-mat].
- [18] R. Yusupov, T. Mertelj, V. V. Kabanov, S. Brazovskii, P. Kusar, J.-H. Chu, I. R. Fisher, and D. Mihailovic, *Nature Physics* **6**, 681 (2010).
- [19] P. Kusar, J. Demsar, D. Mihailovic, and S. Sugai, *Physical Review B* **72**, 014544 (2005).
- [20] P. Kusar, V. V. Kabanov, S. Sugai, J. Demšar, T. Mertelj, and D. Mihailović, *Journal of Superconductivity and Novel Magnetism* **24**, 421 (2010).
- [21] For maximum accuracy we subtract signal at $\Delta t_{\text{D-P}} = 0.2$ ps after the D pulse at 34 K (6 K above T_c). This allows to completely separate pseudogap from superconducting signal and give a good estimate for remaining signal at timescales up to 1 ps.
- [22] For the analysis of the relaxation time the dataset at $\Delta t_{\text{D-P}} = 0$ is subtracted. This allows to remove the long-lived contribution after τ_{th} , which originates in pump induced heating and is independent on $\Delta t_{\text{D-P}}$.
- [23] V. V. Kabanov, J. Demsar, B. Podobnik, and D. Mihailovic, *Physical Review B* **59**, 1497 (1999).
- [24] I. K. Schuller and K. E. Gray, *Journal of Superconductivity and Novel Magnetism* **19**, 401 (2006).
- [25] I. Madan, T. Kurosawa, Y. Toda, M. Oda, T. Mertelj, P. Kusar, and D. Mihailovic, *Scientific reports* **4**, 5656 (2014).
- [26] L. Gor'kov and N. Kopnin, *Uspekhi Fizicheskikh Nauk* **116**, 413 (1975).
- [27] M. Suzuki and M. Hikita, *Physical Review B* **44**, 249 (1991).
- [28] L. Perfetti, P. a. Loukakos, M. Lisowski, U. Bovensiepen, H. Eisaki, and M. Wolf, *Physical Review Letters* **99**, 197001 (2007).
- [29] B. Mansart, D. Boschetto, A. Savoia, F. Rullier-Albenque, F. Bouquet, E. Papalazarou, A. Forget, D. Colson, A. Rousse, and M. Marsi, *Physical Review B* **82**, 024513 (2010).
- [30] H.-H. Wen, Z.-Y. Liu, F. Zhou, J. Xiong, W. Ti, T. Xiang, S. Komiya, X. Sun, and Y. Ando, *Physical Review B* **70**, 214505 (2004).
- [31] A. Junod, A. Bezinge, D. Cattani, J. Cors, M. Decroux, Ø. Fischer, P. Genoud, L. Hoffmann, J.-L. Jorda, J. Muller, and E. Walker, *Japanese Journal of Applied Physics* **26**, 1119 (1987).
- [32] L. Stojchevska, P. Kusar, T. Mertelj, V. V. Kabanov, Y. Toda, X. Yao, and D. Mihailovic, *Physical Review B* **84**, 180507 (2011).
- [33] V. V. Baranov and V. V. Kabanov, *Physical Review B* **89**, 125102 (2014).
- [34] Z. Xu, N. Ong, Y. Wang, T. Kakeshita, and S. Uchida, *Nature* **406**, 486 (2000).
- [35] A. Junod, M. Roulin, B. Revaz, and A. Erb, *Physica B: Condensed Matter* **280**, 214 (2000).
- [36] J. Corson, R. Mallozzi, and J. Orenstein, *Nature* **398**, 221 (1999).
- [37] L. Perfetti, B. Sciollo, G. Birollo, C. van der Beek, C. Pivovera, M. Wolf, and T. Kampfrath, *Physical Review Letters* **114**, 1 (2015).
- [38] G. E. Volovik, *Physica B: Condensed Matter* **280**, 122 (2000).
- [39] In the original paper the misprint occurred - the power of the fraction was 1/8 instead of 3/8.